Size-Dependent Accumulation of the Mitotic Activator Cdc25 as a Mechanism of Size Control in Fission Yeast

Daniel Keifenheim[1], Xi-Ming Sun[2,3], Edridge D'Souza[1], Makoto Ohira[1], Mira Magner[1], Michael Mayhew[4], Samuel Marguerat[2,3], Nicholas Rhind[1,5]

1) Department of Biochemistry and Molecular Pharmacology, University of Massachusetts Medical School, Worcester MA USA
2) MRC Clinical Sciences Centre, London UK
3) Institute of Clinical Sciences, Faculty of Medicine, Imperial College London, London UK
4) Lawrence Livermore National Laboratory, Livermore CA USA
5) Corresponding Author: nick.rhind@umassmed.edu

Abstract

Proper cell size is essential for cellular function (Hall et al., 2004). Nonetheless, despite more than 100 years of work on the subject, the mechanisms that maintain cell size homeostasis are largely mysterious (Marshall et al., 2012). Cells in growing populations maintain cell size within a narrow range by coordinating growth and division. Bacterial and eukaryotic cells both demonstrate homeostatic size control, which maintains population-level variation in cell size within a certain range, and returns the population average to that range if it is perturbed (Marshall et al., 2012; Turner et al., 2012; Amodeo and Skotheim, 2015). Recent progress has revealed two different strategies for size control: budding yeast uses an inhibitor-dilution strategy to regulate size at the G1/S transition (Schmoller et al., 2015), while bacteria appear to use an adder strategy, in which a fixed amount of growth each generation causes cell size to converge on a stable average (Campos et al., 2014; Jun and Taheri-Araghi, 2015; Taheri-Araghi et al., 2015; Tanouchi et al., 2015). Here we present evidence that cell size in the fission yeast *Schizosaccharomyces pombe* is regulated by a third strategy: the size dependent accumulation of the mitotic activator Cdc25. Cdc25 is transcriptionally regulated such that smaller cells accumulate less Cdc25 and larger cells accumulate more Cdc25, creating an increasing concentration of Cdc25 as cell grow and providing a mechanism for cells to trigger cell division when they reach a threshold concentration of Cdc25. Since regulation of mitotic entry by Cdc25 is well conserved, this mechanism may provide a wide spread solution to the problem of size control in eukaryotes.

Results and Discussion

Size control in fission yeast is regulated by coordinating the timing of mitotic entry with cell size (Fantes, 1977). Fission yeast specific hypotheses that rely on cellular geometry have been proposed for this coordination (Martin and Berthelot-Grosjean, 2009; Moseley et al., 2009), but, in the absence of these mechanisms, cells maintain size homeostasis (Wood and Nurse, 2013; Bhatia et al., 2014), demonstrating that other size-control mechanisms exist. The cell cycle machinery that regulates the entry into mitosis in fission yeast and other eukaryotes is well understood (Morgan, 2006), so we looked there for potential regulators of cell size. Cdc25—the tyrosine phosphatase that dephosphorylates tyrosine 15 (Y15) of Cdc2, the catalytic subunit of the fission yeast cyclin-dependent kinase (CDK)—is an attractive candidate. Y15 dephosphorylation of Cdc2 is the rate-limiting step for entry into mitosis (Gould and Nurse, 1989) and Cdc25 has been proposed to be involved in cell-size regulation (Moreno et al., 1990). Its activity is balanced by Wee1, which phosphorylates Cdc2-Y15 (Russell and Nurse, 1987). We hypothesized that Cdc25, accumulating in a size-dependent manner, would trigger entry into mitosis only when it reaches a certain threshold, ensuring that small cells stayed in G2 and only sufficiently large cells enter mitosis. Specifically, we propose that the concentration of Cdc25 increases linearly with size and thus the amount of Cdc25 in the cell, which is the concentration times the cell size, would increase as the square of size. Such protein accumulation is unusual, since most proteins maintain a constant concentration as cells grow (Newman et al., 2006).

To test our hypothesis, we measured the relative concentrations of Cdc25 in synchronous cultures, using the metabolic protein Ade4 as an internal control. During G2, the concentration of Cdc25 increases about 2 fold (Figure 1A), consistent with our hypothesis. In contrast Wee1, assayed in the same manner, maintains a relatively constant concentration during G2 leading to an increasing Cdc25/Wee1 ratio as cell increase in size (Figures 1A and 1B). Both Cdc25 and Wee1 are unstable in G1 (Creanor and Mitchison, 1996; Aligue et al., 1997; Wolfe and Gould, 2004), resetting the system for the next G2.

We next examined the dynamic range of Cdc25 size-dependent accumulation. We arrested cells in G2 with a temperature-sensitive allele of *cdc2* and measured the concentration of Cdc25 relative to Wee1 as cells grew from a normal size of around 15 μm to over three times that size. As cells grew, Cdc25 concentration increased linearly with size (Figure 1C), showing that it is an accurate measure of cell size well beyond the normal length of G2.

To confirm the bulk analysis of Cdc25 concentration, we analyzed the accumulation of Cdc25-NeonGreen in individual cells. As previously reported for Cdc25-GFP (Lu et al., 2012), Cdc25-NeonGreen signal increases with size (Figure 1D).

We tested if the size-dependent accumulation of Cdc25 was regulated transcriptionally by measuring steady-state transcript levels. Mirroring protein levels, the concentration of *cdc25* transcript raises about 2 fold during G2 (Figure 2A). Furthermore, we see a similar increase in *cdc25* transcripts at the single cell level (Figure 2B). *cdc25* transcript number, as assayed by single-molecule RNA-FISH (smFISH), increases faster than cell size. When including the entire dataset, the *cdc25* data is best fit by an increase of $y=x^{1.53}$, significantly higher than the rbp1 control ($y=x^{0.98}$, $p < 10^{-10}$, t test). Furthermore, when cells in the normal range of sizes are analyzed, they are fit by $y=x^{1.86}$, much closer to the predicted increase of $y=x^2$, consistent with the previous reports of larger cells being limited in their ability to maintain transcription homeostasis (Zhurinsky et al., 2010). Importantly, the *cdc25* data is not well fit by a constant concentration model, which predicts $y=x^1$ for normalized transcript data.

We considered two explanations for the increase in the concentration of the *cdc25* transcript and its protein product during G2. The first explanation is that *cdc25* is turned on in early G2 and accumulates with pre-steady-state kinetics without reaching an expression equilibrium before cells enter mitosis. In such a model, the increases in Cdc25 concentration is time-dependent, not size-dependent. The second explanation is that Cdc25 protein is expressed at a size-dependent steady state throughout G2, and thus serves as a direct measure of cell size. It is possible to distinguish between pre-steady-state accumulation and size-dependent accumulation by examining the half live of the Cdc25 protein and its transcript. The time it takes a protein to come to equilibrium after an increase in transcription is determined by the half life of the protein and its transcript (Mehra et al., 2003; Belle et al., 2006). Therefore, for Cdc25 to accumulate in pre-steady-state kinetics for the approximately 2 hour fission yeast G2 (or for the 3 hours it accumulated in Figure 1C), it would have to have transcript or protein half life on the order of hours. On the contrary, we find that the half life of Cdc25 protein is about 15 minutes (Figure 2C) and the half life of the *cdc25* transcript is about 7 minutes (Figure 2D), consistent with previously reported data (Eser et al., 2016). These results demonstrate that Cdc25 levels do not increase in G2 due to pre-steady-state accumulation and supports a model in which Cdc25 concentrations increases at a size-dependent equilibrium.

Size control by size-dependent accumulation of an unstable mitotic activator has been proposed in a number of eukaryotic systems, including fission yeast, protists and mammalian cells (Miyamoto et al., 1973; Herring, 1974; Fantes et al., 1975; Polanshek, 1977; Tyson et al., 1979; Wheals and Silverman, 1982). A hallmark of this mechanism of size control is the phenomenon of excess mitotic delay, in which short pulses of the protein-synthesis inhibitor cycloheximide cause longer mitotic delays the closer they are applied to mitosis (Mitchison, 1971). These results have been interpreted in the context of the unstable-activator hypothesis. This hypothesis posits that cell size is regulated by the size-dependent accumulation of an unstable mitotic activator, which triggers mitosis when it reaches a critical threshold in late G2. Since the activator rapidly decays during short G2 pulses of cycloheximide, a pulse in early G2 allows cells sufficient time to resynthesize the activator before mitosis, but a pulse applied later in G2 provides insufficient time for the activator to be resynthesized, thus delaying mitosis.

Fission yeast exhibit excess mitotic delay in response to cycloheximide pulses (Herring, 1974; Polanshek, 1977). Our results suggest that Cdc25 is an unstable activator that regulates cell size in fission yeast. To test if Cdc25 behaves as predicted by the unstable-activator model, we measured the kinetics of Cdc25 degradation and reaccumulation during and after a cycloheximide pulse. As predicted, Cdc25 levels fall during the pulse and then return to pre-pulse levels (Figure 3A). Importantly, the cycloheximide-treated cells do not divide until Cdc25 recovers to the level at which untreated cells divide (Figure 3A) and the delay in Cdc25 recovery matches the delay in mitotic entry (Figures 3A,B), suggesting that recovery of Cdc25 to a critical threshold is required to trigger the G2/M transition.

Our model makes specific predictions about the role of Cdc25 expression kinetics in triggering the G2/M transition. To test if these predictions are consistent with the detailed understanding of the G2/M regulatory network (Morgan, 2006), we integrated our hypotheses into a quantitative model fission yeast cell-cycle dynamics (Novak and Tyson, 1995). We modified the model to include size-dependent increase in Cdc25 concentration and found realistic parameters under which such an increase was sufficient to drive stable cell cycles (Figure 4A) and to maintain size homeostasis (Figures 4B,C). We then simulated the effect of cycloheximide pulses on the system and found that it recapitulated the excess delay phenomenon

(Figure 4D), in agreement with our experimental data (Figure 4E). This model-based analysis demonstrates that size-dependent accumulation of Cdc25 provides a plausible mechanism for size control in fission yeast and accounts for the excess delay phenomena seen in fission yeast and other eukaryotes.

Our data and analysis support a model in which size-dependent transcription of Cdc25 leads to size-dependent accumulation of this mitotic inducer and thus size-dependent entry into mitosis. When cells are small, the activity of Cdc25 is insufficient to dephosphorylate and activate the Cdc2 CDK. When cells reach a critical size, the concentration of Cdc25 increases to the point at which it can begin to dephosphorylate Cdc2, which in turn hyper-activates Cdc25, fully dephosphorylating Cdc2 and committing cells to mitosis (Lu et al., 2012). Because the Cdc25 phosphatase and its CDK substrates are well-conserved across fungi and metazoa (Morgan, 2006), size-dependent expression of Cdc25 provides a potentially wide-spread solution for the question of size control in eukaryotes.

Experimental Procedures

Cell Culture

Strains were created and cultured using standard techniques (Forsburg and Rhind, 2006). Cells were grown in yeast extract plus supplements (YES) at 30°C, unless otherwise noted. Strains with temperature-sensitive alleles were grown at 25°C for permissive growth and switched to 35°C for non-permissive growth. The follow in strains were used.

yFS105	h- leu1-32 ura4-D18
yFS145	h+ leu1-32 ura4-D18 wee1::pWAU-50 (adh:wee1-50 ura4)
yFS810	h- leu1-32 ura4-D18 ade4-Bluc (KanMX) wee1-Rluc (NatMX)
yFS870	h- leu1-32 ura4-D18 wee1-Rluc (NatMX) cdc25-luc (KanMX)
yFS874	h- leu1-32 ura4-D18 ade4-Rluc (NatMX) cdc25-luc (KanMX)
yFS893	h- leu1-32 ura4-D18 cdc2-L7 wee1-Rluc (NatMX) cdc25-luc (KanMX)
yFS971	h- leu1-32 ura4-D18 cdc2-33 cdc25-NeonGreen (HygMX)

Synchronization and Time Course

Cells were synchronized by centrifugal elutriation in a Beckman JE-5.0 elutriating centrifuge (Willis and Rhind, 2011). Time points were taken every 20 minutes to measure septation and for protein samples. Septation was monitored by counting unseptated, septated, and undivided pairs. Mitotic index was calculated as the ratio of septated and undivided pairs divided by total count for that time point. For luciferase assays, samples were washed with cold water, pelleted and frozen in liquid nitrogen.

Luciferase Assay

Cell pellets were assayed luciferase activity following a modified procedure based on the Dual-Luciferase Reporter Assay (Promega, Madison WI). 5-10 OD pellets were lysed at 4˚C in 200 µl 1X Passive Lysis Buffer by bead beating to a point where ~80% of the cells were lysed. Lysates were cleared at 16,000 g at 4°C. 10 µl of cleared lysate was loaded per well in a 96-well plate and each sample was read in triplicate at room temperature. For each well, 50 µL of Luciferase Assay Substrate and Stop and Glow Buffer are added sequentially to assay for beetle followed by Renilla luciferase. After the addition of each Substrate, the samples rest for 2 seconds followed by a 10 second measurement for luminescence.

Microscopy
Cells were imaged on an DeltaVision OMX microscope with a 60x/1.42 NA objective and InSightSSI solid-state fluorescence illumination. Images were manually analyzed using ImageJ 1.49q (Schneider et al., 2012).

Transcript Quantitation
For NanoString quantitation, $1x10^7$ cells were fixed with 70% methanol and stored at -80°C in 1 ml of RNALater (Ambion). For processing, cells were pelleted, resuspended in 600 µl RLT buffer (Qiagen) with 1% β-mercaptoethanol and lysed by bead beating. 200 µl of lysate was cleared at 16,000 g and 3 µl of supernatant was processed on a NanoString nCounter (Seattle, WA) according to the manufacturers instructions.

Single molecule RNA Fluorescence In Situ Hybridization (smFISH), aImaging and Quantification
smFISH samples were prepared according to a modification of published protocols (Trcek et al., 2012; Heinrich et al., 2013). Briefly, cells were fixed in 4% formaldehyde and the cell wall was partially digested using Zymolyase. Cells were permeabilized in 70% EtOH, pre-blocked in BSA and salmon sperm DNA, and incubated over-night with custom Stellaris oligonucleotides sets (Biosearch Technologies) designed against cdc25 (CAL Fluor® Red 610) and rpb1 (Quasar® 670) mRNAs. Cells were mounted in ProLong Gold antifade reagent with DAPI (Life Technologies) and imaged on a Leica TCS Sp8 confocal microscope, using a 63x/1.40 oil objective. Optical z sections were acquired (z-step size 0.3 microns) for each scan to cover the depth of the cells. Cell boundaries were outlined manually in ImageJ and single mRNA molecules were identified and counted using the FISH-quant MATLAB package (Mueller et al., 2013). Cell area, length and width were quantified using custom-made ImageJ macros. The FISH-quant detection technical error was estimated at 6-7% by quantifying rpb1 mRNAs simultaneously with two sets of probes labeled with different dyes.

Transcript Half Life and RT-qPCR
For calculation of transcript half-life, log phase cultures were treated with 15 µg/ml thiolutin to inhibit polymerase II and 10 OD samples were taken at 0, 5, 10 and 30 minutes. Samples were pelleted and frozen in liquid nitrogen. Total RNA was isolated from pellets using the Direct-zol kit (Zymo Research, Irvine, CA). First strand synthesis was performed using random hexamers and SuperScript III first strand synthesis kit (Invitrogen). qPCR was performed using Kappa SYBR Fast qPCR kit (Wilmington, MA). Transcripts were normalized to 0 time point and *srp7* as an internal control for a stable transcript. Primers for each target are as follows:
cdc25 - ATGACCTGCACCAAGGCTAT, TCATTAACGTCTGGGGAAGC
wee1 - GATGAGGTTTGCTGGGTTGA, CATTCACCTGCCAATCTTCC
cdc13 - ACCACGAGCTGTCCTTAACC, TGCTTAACCGACCAGGTTCC
upf2 - ATCCGCCAAAGCGTGGTATC, AAGCGCACTAAGCAGACGAG
srp7 - GTGCATGTTCGGTGGTCTCG, AAGACCCGGTAGTGATGTGC.
Half life data was fit with an exponential curves using Igor Pro (WaveMetrics).

Excess Delay Assay and Protein Half Life
To measure protein half lives, strains with a luciferase-tagged protein of interest were grown to log phase, 100 µg/ml of cycloheximide was added and 10 OD samples were taken at 0, 5, 10 and 30 minutes. Samples were pelleted, frozen in liquid nitrogen and processed as described above

for luciferase measurement. Half life data was fit with an exponential curve using Igor Pro (WaveMetrics).

To assay for excess delay, an elutriation time course, described above, was modified by splitting the synchronized culture into two subcultures. One subculture was treated with a 20 minute pulse of 100 μg/ml of cycloheximide. Cycloheximide was removed by filtration and cells were put into fresh media and sampled for septation and luciferase activity.

Replicating the Novak and Tyson fission yeast cell cycle model

We based our model on that of Novak and Tyson, which we refer to as NT95, consisting of 18 differential equations and ~50 rate constant parameters (Novak and Tyson, 1995). In NT95, cell size is regulated by the activation of Wee1 inhibitory phosphorylation upon the attainment of a critical cell size. Thus, as the cell grows over the course of the cell cycle and active MPF levels rise, Wee1 remains active, and cells remain in G2. At the appropriate cell size, upstream kinases are activated, inhibiting Wee1, leading to Cdc2 dephosphorylation and mitotic entry. In this model, Cdc25 concentration is not size-dependent. It is also worth noting that G1/S progression is modeled by a "black box" automata in which certain rate constant parameters are set to different values depending on whether the cell has reached a certain size or on whether a certain amount of time has elapsed since division (Novak and Tyson, 1995). As the G2/M transition is the focus of our work, we retained this automata model for G1/S progression. The model was fully implemented in MATLAB; the code is available upon request.

We obtained initial conditions by simulating from the model with the growth rate set to 0, taking the values of all species once they appeared to equilibrate (after ~5 cycles). Rate constant values were taken directly from NT95. Cell growth was assumed to be exponential with a mass doubling time fixed at 180 minutes. Simulations were generated with MATLAB's `ode15s` solver (variable order, multistep) for stiff systems of ODEs.

To test that the model had been successfully replicated, we recreated Table 1 from NT95, simulating from our version of NT95 and estimating the proportion of time spent in each part of the cell cycle under the 21 different genetic conditions tested. All our estimates corresponded exactly to those in Table 1 of NT95.

Modifying and fitting the wild-type fission yeast cell cycle model

We modified the NT95 model by removing the size dependence from the Wee1 edges of the biochemical network, instead making total Cdc25 concentration dependent on cell mass. Namely,

$$\frac{d}{dt}[total\ Cdc25] = k_{syn}[mass] - k_{deg}[total\ Cdc25]$$

To estimate rate constants for the wild-type model, we first simulated for three cycles from the original NT95 model. We then treated these simulated curves for each species as data. Assuming that the rate constants for the modified model, which we refer to as SC15, would not be too far removed from their previous values, we used a direct, pattern search optimization routine to estimate rate parameters for our wild-type SC15 model. We used the sum of squared errors between three-cycle simulations from our SC15 model and the three-cycle simulations generated by the NT95 model as our objective function. All species were compared in this optimization. To constrain the optimization, we used lower bounds of 0 and upper bounds of 10 times the NT95 values of each rate parameter. The values of nearly every rate constant in the

SC15 model remained unchanged from their NT95 values. Estimates for rate constants in the SC15 model that differed are shown below:

Parameter	Description	NT95 Value	SC15 Value
k_3	Formation of unphosphorylated MPF	10.0	6.125
k_{CAK}	Phosphorylation of Cdc2 threonine	1.0	1.25
k_a	Phospho-activation of Cdc25	0.5	0.75
k_{d1}	Dephosphorylation (N-terminal) of Wee1	1.0	4.0
k_{w1}	Phosphorylation (N-terminal) of Wee1	1.0	4.5312
k_{d2}	Dephosphorylation (C-terminal) of Wee1	1.0	1.25
k_u	Activation of Mik1 by unreplicated DNA	2.0	4.0
k_{ui}	Degradation of Mik1	0.2	0.7
K_{m1}	Half-saturating constant for MPF phosphorylation	1.0	1.125
K_d	Half-saturating constant for W deactivation	0.05	0.3
K_e	Half-saturating constant for UbE activation	0.01	0.0725
V_{wee}''	Component of k_{wee} parameter for MPF phosphorylation	0.75	0.7344
F_d	Multiplier of W for Cdc25 deactivation	2.0	3.0

Simulating cycloheximide-pulse experiments

To simulate the cycloheximide-pulse experiments, we introduced a new terminal event representing the pulse to interrupt the ODE solver. The two parameters of the pulse were the time post-G2 entry (in minutes) at which the pulse occurred and the duration of the pulse. The duration of the pulse was fixed to 20 minutes in all simulations while we varied the start time of the pulse from 0 to 120 minutes post-G2 entry (by 20 minutes). At the onset and for the duration of the pulse, the Cdc25 synthesis rate constant (k_{syn}) was set to 0.0. The Cdc25 synthesis rate was restored to its original value after the pulse. We only generated one pulse per simulation, and we recorded effects of the pulse on cell-cycle duration and mass at division.

Author Contributions

Conceptualization: DK,NR; Methodology: DK,XS,ED,MO,MM,SM,NR; Software: ED,MM; Formal Analysis: DK,MM,SM,NR; Investigation: DK,XS,ED,MO,MM,AH,MM,NR; Data Curation: NR; Writing–Original Draft: NR; Writing–Review & Editing: DK,XS,ED,MO,MM,AH,MM,SM,NR; Visualization: DK,SM,NR; Supervision: SM,NR; Project Administration: NR; Funding Acquisition: SM,NR

Acknowledgements

We are grateful to Jenny Benanti, Dan McCollum, Peter Pryciak, and members of the Benanti and Rhind labs for insightful suggestions on this work and constructive comments of the manuscript and to Alan Herring and Murdoch Mitchison their pioneering work on the excess-delay phenomena in fission yeast. This work was supported by GM098815 to NR and the UK Medical Research Council to SM.

Figure Legends

Figure 1: Cdc25 accumulates in proportion to cell size.
(A) Cdc25 protein concentration doubles during G2. Cells expressing Cdc25-Rluc and Ade4-Bluc from their endogenous loci (yFS874) were elutriation synchronized in early G2 and followed through two synchronous cell cycles. Samples were taken every 20 minutes for luciferase quantitation and examined microscopically for septation. As a comparison, cells expressing Wee1-Rluc and Ade4-Bluc (yFS810) were similarly assayed. The midpoint of septation for each cycle is marked with an arrowhead and the inferred M-G1-S phases of the cycles are indicated in gray. The mean and standard error of the Ade4-nomalized Cdc25 and Wee1 signal, relative to time 0, is shown. n=3.
(B) The Cdc25/Wee1 protein ratio doubles during G2. Cells expressing Cdc25-Bluc and Wee1-Rluc (yFS870) were assayed as in **a**. n=3.
(C) The Cdc25/Wee1 protein ratio increases linearly with cell size. *cdc2-ts* cells expressing Cdc25-Bluc and Wee1-Rluc (yFS893) were shifted to the restrictive temperature of 35˚C and sampled every 20 minutes. A transient increase in the Cdc25/Wee1 ratio was reproducibly seen after temperature shift. n=2.
(D) Cdc25 protein concentration increases linearly with cell size. *cdc2-ts* cells expressing Cdc25-NeonGreen (yFS971) were shifted to the restrictive temperature of 35˚C and sampled at 0, 2 and 4 hours. Cdc25-NeonGreen signal and cell length were measured microscopically in individual cells. The concentration of Cdc25 was calculated as the total Cdc25-NeonGreen signal divided by the cell size.

Figure 2: Cdc25 accumulation is regulated by transcript synthesis.
(A) *cdc25* transcript concentration doubles during G2. Wild-type cell (yFS105) were elutriation synchronized in early G2 and followed through two synchronous cell cycles. Samples were taken every 20 minutes for RNA quantitation and examined microscopically for septation. Steady-state mRNA levels were determined using the NanoString nCounter method with custom probes and normalized to total mRNA counts. Data points represent independent biological replicates, the lines connect the mean of those points. For the first two hours, n=2, for the rest of the time course, n=1.
(B) Cdc25 transcript concentration increase as individual cells grow. *adh1:wee1-50ts* cells (yFS145), which arrest in G2 at 25˚C due to Wee1 over expression, but are wild type at 35˚C where the overexpressed, temperature-sensitive allele of Wee1 is inactive, were shifted to the restrictive temperature of 25˚C and sampled at 0, 2 and 4 hours. Cells were simultaneously analyzed for *cdc25* and *rbp1* transcript number by single-molecule RNA FISH. The data was fit with $y=x^a$; for *cdc25*, data from cells from 1 to 2 fold relative size was also fit. Relative size is reported because size was measured as cell area.
(C) Cdc25 protein is unstable. Cells expressing Cdc25-Rluc and Ade4-Bluc (yFS874) were treated with 100 µg/ml cycloheximide and sampled as indicated for luciferase quantitation. As a comparison, cells expressing Wee1-Rluc and Ade4-Bluc (yFS810) were similarly assayed. The mean and standard error of the Ade4-nomalized Cdc25 and Wee1 signal, relative to time 0, is shown. n=3 for Cdc25; n=2 for Wee1.
(D) *cdc25* transcript mRNA is unstable. Wild-type cells (yFS105) were treated with 15 µg/ml thiolutin and sampled as indicated for RNA quantitation by qRT-PCR. The mean and standard error, relative to time 0, is shown. n=3.

Figure 3: Cdc25 behaves as an unstable activator of mitosis.
(A) The delay in Cdc25 accumulation after a cycloheximide pulse mirrors the delay in mitotic entry. Cells expressing Cdc25-Bluc and Wee1-Rluc (yFS870) were elutriation synchronized in early G2; samples were taken every 20 minutes for luciferase quantitation and examined microscopically for septation. At the indicated times before division of the untreated cells, the culture was split and one half was treated with 100 µg/ml cycloheximide for 20 minutes.
(B) Quantitation of cycloheximide-induced delay in Cdc25 accumulation and mitotic entry. Data from twelve experiments conducted as described in (A) is displayed. The experiments in (A) are shown as circles.

Figure 4: Mathematical modeling of cell-size control by Cdc25 accumulation.
(A) Cdc25 concentration regulated model of the cell cycle. Simulation of the cell cycle using an ordinary differential equation model in which the size-dependent accumulation of Cdc25 triggers entry into mitosis at the appropriate size.
(B) The cell cycle simulated as in (A), but initialized with a cell half the normal size at mitosis.
(C) The cell cycle simulated as in (A), but initialized with a cell twice the normal size at mitosis.
(D) Simulation of cycloheximide-induced delay in Cdc25 accumulation and mitotic entry. The cell cycle simulated as in (A), but with a simulated pulse of cycloheximide, during which the synthesis of Cdc25 is set to 0, between 120 and 140 minutes (60 and 40 minutes before cell division would have happened without the pulse).
(E) Quantitation of cycloheximide-induced delay simulations. The simulation in (D) was run with simulated cycloheximide pulses at various times from 20 to 140 minutes before cell division would have occurred in an untreated cell. For each simulation, the extent of cell cycle delay was recorded and plotted against time of the pulse.

References

Aligue, R., Wu, L., and Russell, P. (1997). Regulation of Schizosaccharomyces pombe Wee1 tyrosine kinase. J Biol Chem *272*, 13320-13325.

Amodeo, A. A., and Skotheim, J. M. (2015). Cell-Size Control. Cold Spring Harb Perspect Biol

Belle, A., Tanay, A., Bitincka, L., Shamir, R., and O'Shea, E. K. (2006). Quantification of protein half-lives in the budding yeast proteome. Proc Natl Acad Sci U S A *103*, 13004-13009.

Bhatia, P., Hachet, O., Hersch, M., Rincon, S. A., Berthelot-Grosjean, M., Dalessi, S., Basterra, L., Bergmann, S., Paoletti, A., and Martin, S. G. (2014). Distinct levels in Pom1 gradients limit Cdr2 activity and localization to time and position division. Cell Cycle *13*, 538-552.

Campos, M., Surovtsev, I. V., Kato, S., Paintdakhi, A., Beltran, B., Ebmeier, S. E., and Jacobs-Wagner, C. (2014). A constant size extension drives bacterial cell size homeostasis. Cell *159*, 1433-1446.

Creanor, J., and Mitchison, J. M. (1996). The kinetics of the B cyclin p56cdc13 and the phosphatase p80cdc25 during the cell cycle of the fission yeast *Schizosaccharomyces pombe*. J Cell Sci *109*, 1647-1653.

Eser, P., Wachutka, L., Maier, K. C., Demel, C., Boroni, M., Iyer, S., Cramer, P., and Gagneur, J. (2016). Determinants of RNA metabolism in the Schizosaccharomyces pombe genome. Mol Syst Biol *12*, 857.

Fantes, P. A. (1977). Control of cell size and cycle time in *Schizosaccharomyces pombe*. Journal of Cell Science *24*, 51-67.

Fantes, P. A., Grant, W. D., Pritchard, R. H., Sudbery, P. E., and Wheals, A. E. (1975). The regulation of cell size and the control of mitosis. J Theor Biol *50*, 213-244.

Forsburg, S. L., and Rhind, N. (2006). Basic methods for fission yeast. Yeast *23*, 173-183.

Gould, K. L., and Nurse, P. (1989). Tyrosine phosphorylation of the fission yeast cdc2+ protein kinase regulates entry into mitosis. Nature *342*, 39-45.

Hall, M. N., Raff, M., and Thomas, G. (2004). Cell Growth: Control of Cell Size (Cold Spring Harbor, NY: Cold Spring Harbor Press).

Heinrich, S., Geissen, E. M., Kamenz, J., Trautmann, S., Widmer, C., Drewe, P., Knop, M., Radde, N., Hasenauer, J., and Hauf, S. (2013). Determinants of robustness in spindle assembly checkpoint signalling. Nat Cell Biol *15*, 1328-1339.

Herring, A. J. A Study of the Induced Delay in the Division of Yeast *Schizosccharomyces pombe*. University of Edinburgh; 1974. p. Dissertation.

Jun, S., and Taheri-Araghi, S. (2015). Cell-size maintenance: universal strategy revealed. Trends Microbiol *23*, 4-6.

Lu, L. X., Domingo-Sananes, M. R., Huzarska, M., Novak, B., and Gould, K. L. (2012). Multisite phosphoregulation of Cdc25 activity refines the mitotic entrance and exit switches. Proc Natl Acad Sci U S A *109*, 9899-9904.

Marshall, W. F., Young, K. D., Swaffer, M., Wood, E., Nurse, P., Kimura, A., Frankel, J., Wallingford, J., Walbot, V., Qu, X., and Roeder, A. H. (2012). What determines cell size? BMC Biol *10*, 101.

Martin, S. G., and Berthelot-Grosjean, M. (2009). Polar gradients of the DYRK-family kinase Pom1 couple cell length with the cell cycle. Nature *459*, 852-856.

Mehra, A., Lee, K. H., and Hatzimanikatis, V. (2003). Insights into the relation between mRNA and protein expression patterns: I. Theoretical considerations. Biotechnol Bioeng *84*, 822-833.

Mitchison, J. M. (1971). The Biology of the Cell Cycle (Cambridge: Cambridge University Press).

Miyamoto, H., Rasmussen, L., and Zeuthen, E. (1973). Studies of the effect of temperature shocks on preparation for cell division in mouse fibroblast cells (L cells). J Cell Sci *13*, 889-900.

Moreno, S., Nurse, P., and Russell, P. (1990). Regulation of mitosis by cyclic accumulation of p80cdc25 mitotic inducer in fission yeast. Nature *344*, 549-552.

Morgan, D. O. (2006). The Cell Cycle: Principles of Control (London: New Sciemce Press, Ltd.).

Moseley, J. B., Mayeux, A., Paoletti, A., and Nurse, P. (2009). A spatial gradient coordinates cell size and mitotic entry in fission yeast. Nature *459*, 857-860.

Mueller, F., Senecal, A., Tantale, K., Marie-Nelly, H., Ly, N., Collin, O., Basyuk, E., Bertrand, E., Darzacq, X., and Zimmer, C. (2013). FISH-quant: automatic counting of transcripts in 3D FISH images. Nat Methods *10*, 277-278.

Newman, J. R., Ghaemmaghami, S., Ihmels, J., Breslow, D. K., Noble, M., DeRisi, J. L., and Weissman, J. S. (2006). Single-cell proteomic analysis of S. cerevisiae reveals the architecture of biological noise. Nature *441*, 840-846.

Novak, B., and Tyson, J. J. (1995). Quantitative analysis of a molecular model of mitotic control in fission yeast. Journal of Theoretical Biology *173*, 283 - 305.

Polanshek, M. M. (1977). Effects of heat shock and cycloheximide on growth and division of the fission yeast, Schizosaccharomyces pombe. With an Appendix. Estimation of division delay for S. pombe from cell plate index curves. J Cell Sci *23*, 1-23.

Russell, P., and Nurse, P. (1987). Negative regulation of mitosis by wee1+, a gene encoding a protein kinase homolog. Cell *49*, 559-567.

Schmoller, K. M., Turner, J. J., Koivomagi, M., and Skotheim, J. M. (2015). Dilution of the cell cycle inhibitor Whi5 controls budding-yeast cell size. Nature *526*, 268-272.

Schneider, C. A., Rasband, W. S., and Eliceiri, K. W. (2012). NIH Image to ImageJ: 25 years of image analysis. Nat Methods *9*, 671-675.

Taheri-Araghi, S., Bradde, S., Sauls, J. T., Hill, N. S., Levin, P. A., Paulsson, J., Vergassola, M., and Jun, S. (2015). Cell-size control and homeostasis in bacteria. Curr Biol *25*, 385-391.

Tanouchi, Y., Pai, A., Park, H., Huang, S., Stamatov, R., Buchler, N. E., and You, L. (2015). A noisy linear map underlies oscillations in cell size and gene expression in bacteria. Nature

Trcek, T., Chao, J. A., Larson, D. R., Park, H. Y., Zenklusen, D., Shenoy, S. M., and Singer, R. H. (2012). Single-mRNA counting using fluorescent in situ hybridization in budding yeast. Nat Protoc *7*, 408-419.

Turner, J. J., Ewald, J. C., and Skotheim, J. M. (2012). Cell size control in yeast. Curr Biol *22*, R350-R359.

Tyson, J., Garcia-Herdugo, G., and Sachsenmaier, W. (1979). Control of nuclear division in Physarum polycephalum: Comparison of cycloheximide pulse treatment, uv irradiation, and heat shock. Exp Cell Res *119*, 87-98.

Wheals, A., and Silverman, B. (1982). Unstable activator model for size control of the cell cycle. J Theor Biol *97*, 505-510.

Willis, N., and Rhind, N. (2011). Studying G2 DNA Damage Checkpoints Using the Fission Yeast Schizosaccharomyces pombe. Methods Mol Biol *782*, 1-12.

Wolfe, B. A., and Gould, K. L. (2004). Fission yeast Clp1p phosphatase affects G2/M transition and mitotic exit through Cdc25p inactivation. EMBO J *23*, 919-929.

Wood, E., and Nurse, P. (2013). Pom1 and cell size homeostasis in fission yeast. Cell Cycle *12*,

Zhurinsky, J., Leonhard, K., Watt, S., Marguerat, S., Bahler, J., and Nurse, P. (2010). A Coordinated Global Control over Cellular Transcription. Curr Biol *20*, 2010-2015.

Figure 1

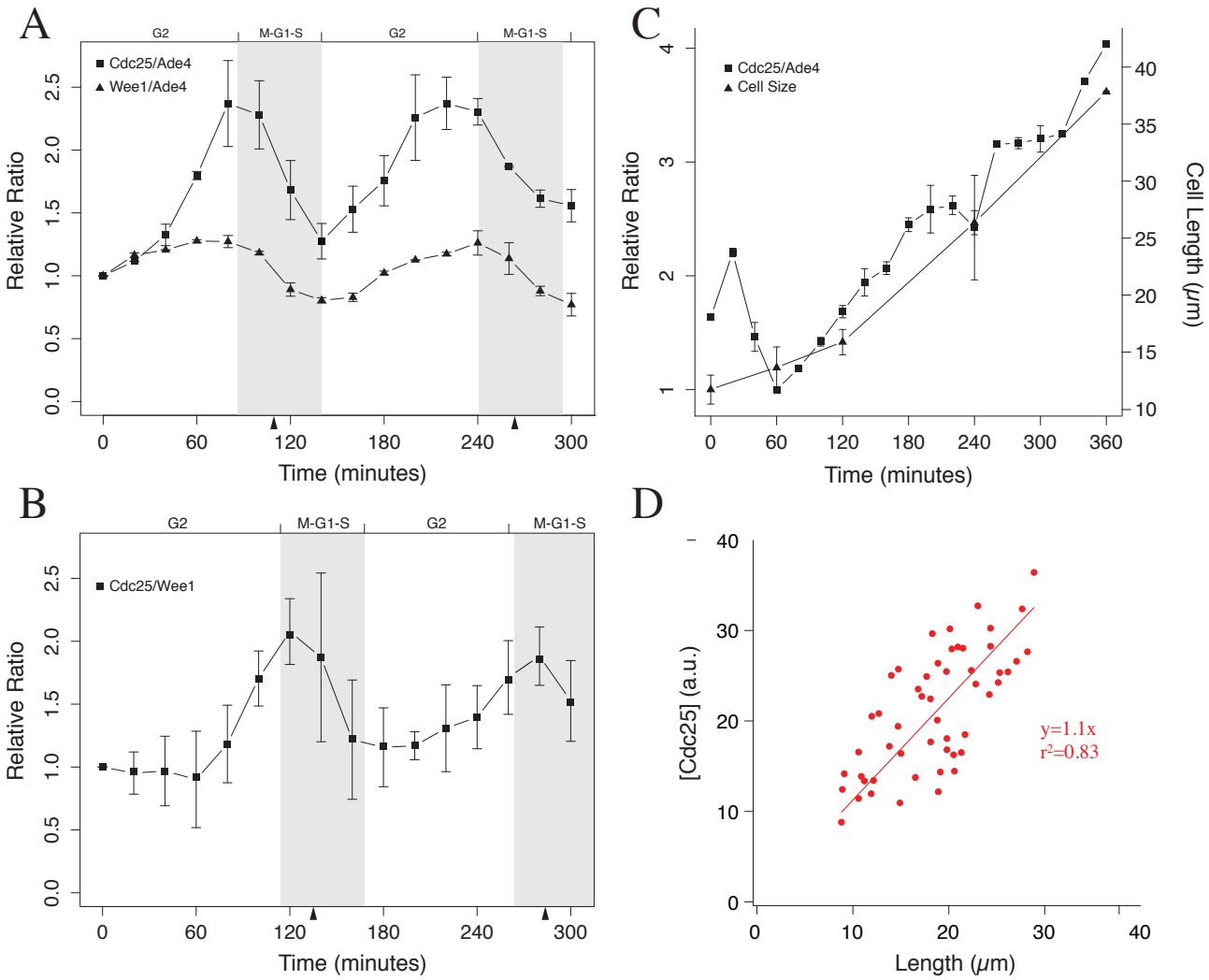

Figure 2

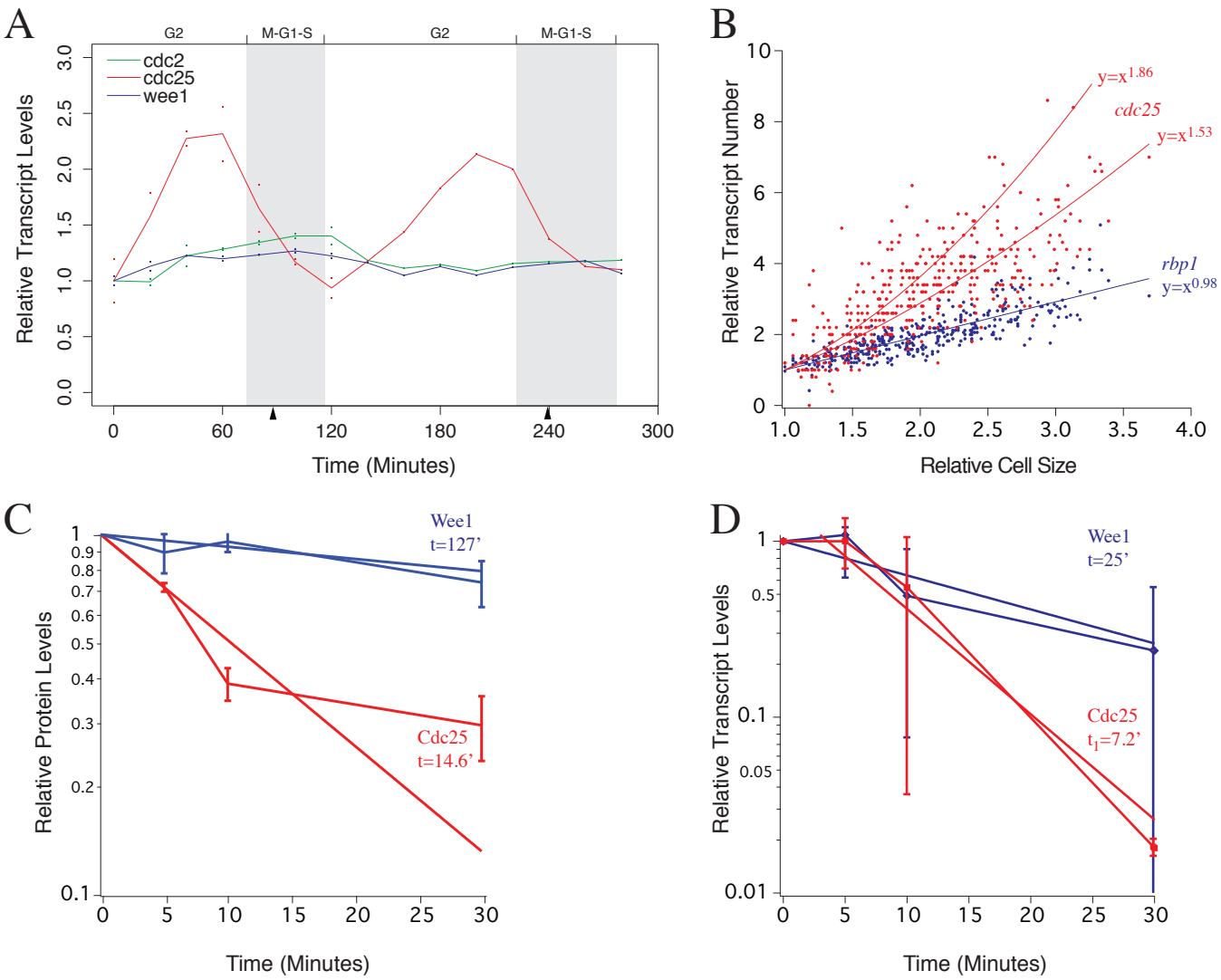

Figure 3

A

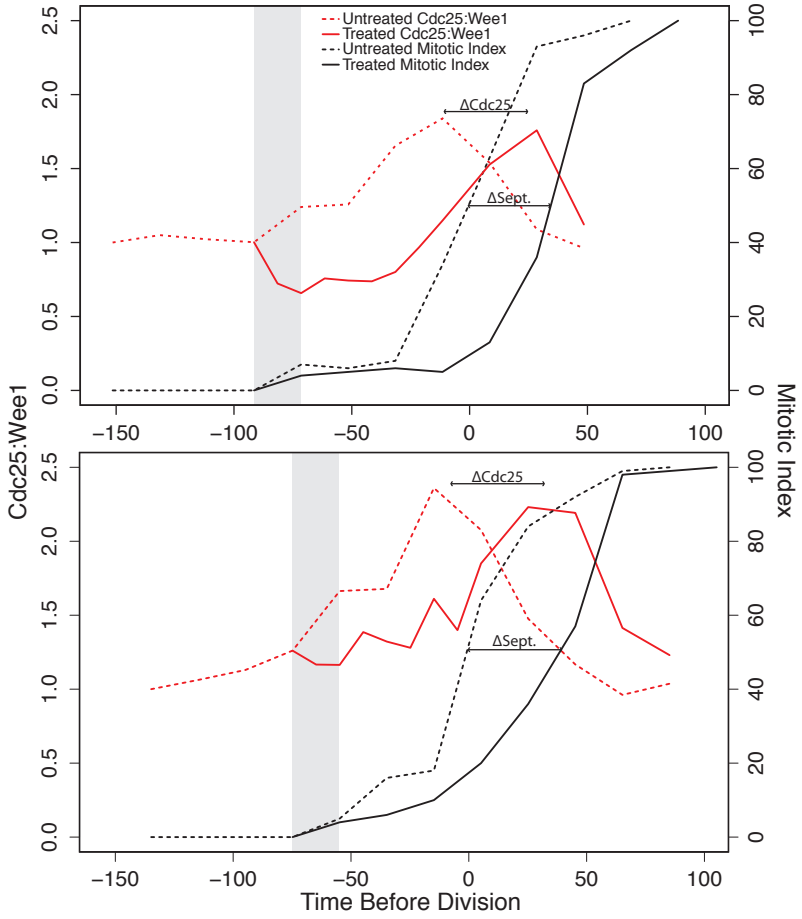

B

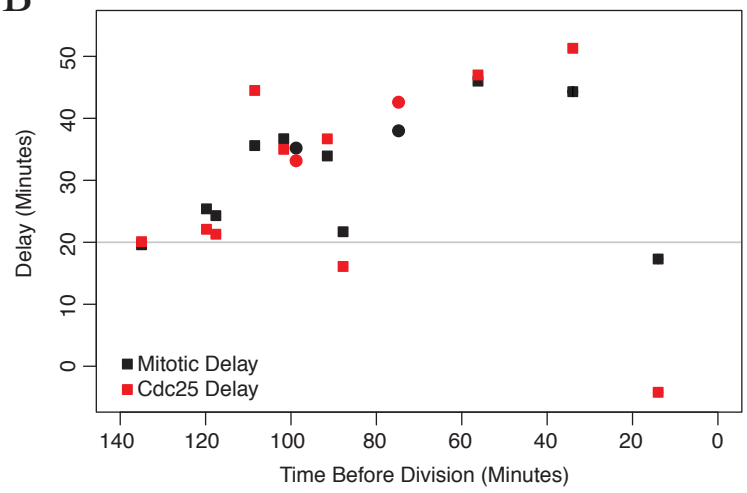

Figure 4